

SPACE WEATHER FORECASTING: UNDER THE HOOD OF THE MAGNETOSPHERIC SPECIFICATION MODEL

R V Hilmer¹, G P Ginet¹, D L Cooke¹, I. Katz²

¹*Air Force Research Laboratory, Space Vehicles Directorate, Hanscom AFB, MA, USA*

²*Science Applications International Corporation, San Diego, CA, USA*

Abstract

The Rice University Magnetospheric Specification Model (MSM) is a space environment model of the inner and middle magnetosphere addressing electron and ion populations relevant to surface charging. The model is driven by geomagnetic indices and geophysical parameters such as the solar wind. With upstream measurements of solar wind conditions present, the successful merging of MSM particle specifications with surface charging algorithms could present the possibility of predicting charging conditions on a spacecraft. Initial comparisons of on-orbit spacecraft frame charging measurements with results obtained by applying a charging algorithm driven by MSM output to a minimum spacecraft description were promising.¹ The method successfully specified the occurrence of the two largest of three spacecraft charging events studied. The goal of this paper is to further explore the efficacy of incorporating the "space weather" simulations of the MSM into a true spacecraft-charging tool. An overview of relevant MSM simulation procedures and recent validation results is given followed by a review of updated MSM/charging algorithm simulations performed using a variety of input parameter combinations. A consistent MSM feature, beneficial to any future spacecraft charging applications, is its ability to balance an ion population with electrons and their evolving spectral features to produce spacecraft charging current densities in the geosynchronous environment.

Introduction

Can a nearly generic spacecraft-charging algorithm be coupled with an environment specification tool such as the Rice University Magnetospheric Specification Model² (MSM)? Interest in this specific topic has grown with the increasing number of attempts to employ the model in anomaly resolution studies. While the MSM does model many parts of the charging environment to which spacecraft are exposed, it does not treat the particles and fields self-consistently and lacks representation of some basic populations such as the cold particles forming the plasmasphere. However, it was designed to be robust enough to run in an operational setting and can be driven solely by the geomagnetic index Kp if data sources are limited. Initial comparisons of on-orbit spacecraft frame charging measurements with results obtained by applying a charging algorithm driven by MSM output to a minimum spacecraft description were promising¹. By running the model in the default Kp -only mode, the method successfully specified the occurrence of the two largest of three spacecraft charging events studied. The basic method involves feeding MSM generated isotropic differential energetic particle fluxes (electrons, H⁺, O⁺) to a spacecraft-charging module that calculates the spacecraft response and whether it will be at risk for hazardous charging. Depending on the availability of solar wind observations, the method could become a standard feature of space environment prediction if successful.

We begin with a review of MSM basics and a brief DSCS data set description, and then an outline of the charging model. Finally, simulation results, derived using three MSM input parameter combinations, are compared with spacecraft charging measurements made in geosynchronous orbit by the Defense Satellite Communication System (DSCS) III.³ The events include the three from the original study¹ plus a large compound magnetic storm event. While the overall results are similar to those of the first study, differences related to input parameter selection are consistent with those anticipated based on validation work involving 20-50 keV electrons and will be useful for determining the optimum model configuration to include in a spacecraft charging tool.

MSM Basics

The Magnetospheric Specification Model² (MSM) describes the 10 eV to 100 keV electron, H⁺, and O⁺ populations of the inner and middle magnetosphere. The cold plasmasphere populations are not addressed in this operational version of the MSM but their inclusion has been investigated⁴. MSM responds to changing geophysical conditions on time scales of 15-30 minutes as described by the geophysical inputs, i.e., magnetic indices Kp and Dst , equatorward boundary of diffuse aurora at midnight (ABI), cross-polar cap potential drop (PCP) and ionospheric convection pattern type (IPT), solar wind (SW) density and velocity, and the IMF. The MSM can be driven by any combination of input

E(keV)	0.03	0.10	0.32	1.00	3.16	10.00	31.62	100.00
Y _{se}	0.23	0.79	1.43	1.11	0.53	0.22	0.10	0.04
Y _{bse}	0.00	0.16	0.26	0.32	0.29	0.24	0.22	0.22
Y _{sp}	0.04	0.04	0.06	0.37	1.25	2.56	3.65	4.00

Table 1. Backscatter and secondary electron yields as a function of energy for incident ions and electrons.

parameters as long as Kp is included. Proxy inputs for absent parameters are generated internally by the model as a function of Kp .

Electron, proton, and oxygen populations are followed separately within a simulation domain extending approximately 10 Re (Earth radii) in the dawn, noon, and dusk directions and out to 20 Re at midnight local time. Species are tracked using defined energy invariants, namely

$$\lambda_s = W_s \left(\int ds/B \right)^{2/3}$$

where W_s is the particle energy in gyrotational and bounce motion and the integral is the volume of a tube containing one unit of magnetic flux. The model follows particles of each selected energy invariant λ_s by assuming that the number of each type per unit magnetic flux with a given energy invariant remains constant along a magnetic flux tube. While the particles are typically energized as they convect earthward, these are the energies the particles have as they pass through the midnight geosynchronous region. A particle tracing routine uses prescribed electric⁵ and magnetic⁶ field models to follow bounce-averaged particle drifts and updates fluxes using Liouville's theorem with corrections for loss. Initial conditions start with statistically based models of fluxes from 2 to 13 Earth radii. Boundary conditions are Kp dependent with more particles entering the outer boundary during active times. While electrons are permitted entry farther toward dusk as PCP increases, boundary particle access is limited in order to keep particles from arriving at geosynchronous orbit with inappropriate energies. Typically, ten invariant energies are tracked for each species, i.e., the values listed in Table 1 along with 10 eV and 200 keV.

Several observed effects are incorporated into MSM simulations that are closely connected to various input parameters. For example, penetration electric fields and the stretching of the night side magnetic field are tied to the motion and value of the ABI. The PCP dictates overall cross-tail electric field strengths. Solar wind pressure (SW) controls the size of the magnetopause while Dst controls the inflation of the inner magnetic field. In turn, all of these properties affect particle motion and their access to parts of the magnetosphere.

Electron fluxes are typically most intense in the midnight-to-dawn local time sector as electrons convect sunward from the magnetotail then grad-curvature drift eastward to orbit about the Earth. Particles can be energized from a few eV to tens of keV by the time they reach geosynchronous altitudes where typical electron fluxes vary in the range 10^4 to 10^7 /cm²/sec/sr/keV as a function of local time and magnetospheric activity.

A recent model validation study² specifically addressed part of the electron population associated with spacecraft charging at geosynchronous altitude. In this study, extended MSM model simulation runs were performed, driven solely by Kp and covering Julian day 1 of 1996 through day 180 of 1998, of 20-50 keV electron flux measurements made by the Charge Control System³ on a DSCS III B-7 spacecraft. A time series sample from this run is shown in the top panel of Figure 1. The comparisons indicate that the model tracks both diurnal and seasonal activity related variations in geosynchronous electrons in a regular and consistent manner regardless of the input parameter subset used as drivers. This feature is essential for the systematic development of operational tools addressing spacecraft charging hazards. No comprehensive validation efforts have addressed H+ or O+.

In addition, MSM simulations were performed using twenty-two permutations of the input parameter set over the extended active period covering days 221-321 of 1996. Distinct characteristics in the temporal responses are evident and can be tied to the type, quality, and frequency of the input parameters as well as the Kp related boundary conditions used by MSM. Figure 1 illustrates a typical range of MSM model behaviors produced. The top panel (MSM02) was produced using the Kp -Only mode and the output often shows significant changes synchronized with the 3-hour cadence of the Kp index. The middle panel (MSM17) represents the low RMS error case (inputs Kp , PCP, SW, and IMF) while the bottom panel (MSM18) represents the high RMS error case (inputs Kp , ABI, SW, and IMF).

While all cases follow the general diurnal flux pattern observed by DSCS, they each respond differently on shorter time scales. In general, runs not using the actual polar-cap potential (PCP) measurement tend to specify higher fluxes and

miss more observed particle dropouts. These runs (e.g., see top and bottom panels of Figure 1) are using a PCP proxy based on Kp , which often means particles arrive at the satellite location early as shown at the beginning of day 273.

DSCS III Flight Data

The Charge Control System³ (CCS) autonomously detects hazardous charging conditions and can actively protect a host spacecraft against differential surface charging effects. CCS was designed to detect hazardous conditions and turn on a plasma source within 1 minute when the source is enabled. The CCS includes an ion electrostatic analyzer (ESA), to measure ions in 31 differential channels between 17 eV and 12.3 keV, for determining frame charging levels and an electron ESA, adapted to measure integral electron counts between 20 keV and 50 keV, for determining the intensity of the frame charging electron population. Two surface potential monitors determine differential charging between material patches and vehicle ground and a plasma generator can autonomously discharge the vehicle prior to excessive charge buildup. The data used in this study were obtained from the ion and electron ESAs on days without operation of the plasma generator. DSCS III B-7 is at 52.5 degrees West longitude, corresponding to 00:00 LT at 03:30 UT. Note that the MSM validation study mentioned above utilized several years of electron ESA observations from this spacecraft.

Spacecraft Charging Model

As in the earlier study¹, an advanced charging code such as NASCAP/GEO⁷ or NASCAP-2K (under development) is not used. Instead, the surface-charging algorithm is separately applied to a minimum spacecraft description. An advantage to this approach is that it becomes easier to differentiate contributions from various MSM simulation configurations and it is easier to determine the minimum degree of spacecraft fidelity needed for space weather forecasting.

Spacecraft charging occurs when the electron flux to spacecraft surfaces exceeds the sum of the fluxes of the electron leaving the surfaces (secondary and backscattered) and the ions hitting the surfaces. The incident electrons are from the magnetosphere. The electron flux from photoemission in sunlight, about $1-4 \times 10^{-5}$ A/m², is greater than any electron flux from the magnetosphere, so spacecraft charging can only occur in sunlight when there are insulating surfaces on a spacecraft. The secondary and backscattered currents are found by integrating the energy and angle dependent incident particle fluxes with yield curves (specifying the ratio of ejected electron to incident particle flux) for the appropriate spacecraft materials. From our experience modeling geosynchronous charging, we use material properties for secondary and backscattered electrons based on laboratory measurements for carbon. As produced by the MSM, the incident fluxes are taken to be isotropic. Photoelectron emission is ignored because electric fields from charged shadowed insulating surfaces suppress the emission of low energy photoelectrons. The backs of the solar arrays on DSCS III are insulating, as is the outer surface of the thermal control blankets, which cover most of the spacecraft body.

Charging is identified as a net electron current to the spacecraft. The net charging current density, I_t , was calculated by integrating the electron, proton, and oxygen fluxes (f_e , f_p , and f_o) over energy using the expression

$$I_t = \pi e \sum \Delta E_i [f_e(E_i)(1 - Y_{se}(E_i) - Y_{bse}(E_i)) - f_p(E_i)(1 + Y_{sp}(E_i)) - f_o(E_i)(1 + Y_{so}(E_i))]$$

where the secondary and backscatter yields are shown in Table 1 for selected energy bins. Owing to the speed difference between a proton and oxygen of a given energy, the secondary electron yields for incident O+, Y_{so} , were assumed to be smaller than those for protons, Y_{sp} , by a factor of 4.

Calculated Currents and Frame Charging

Simulations were run to cover days 45, 215, and 217 of 1996 and days 123 and 124 of 1998. The days were chosen so that there was no CCS plasma source operation and the satellite was not in eclipse. Spacecraft charging ranged from a peak of 200 V negative on day 217, to a peak of 600 V negative on day 215. The 1998 days represent a large compound storm event that did not result in any frame charging on DSCS. The measured spacecraft potential for day 215 of 1996 is shown in Figure 2. Electron, H+, and O+ fluxes at the DSCS location were derived at 15-minute intervals from MSM output. The process involves mapping the two-dimensional simulation results into three dimensions and interpolating in time, space, and invariant energy space to get fluxes for a discrete kinetic energy of interest. To ensure that all MSM particles present were included, the simulation output were sampled at much finer intervals to construct 49 energy “channels” for use in the charging algorithm described above.

Incident and net charging current densities were calculated from the MSM fluxes and material properties using the formula in the preceding section and shown in Figure 2 for three separate runs of day 215. The input parameters used for each run are listed in each panel of the figure. The top panel is basically the Kp -Only case run previously¹. The second panel represents parameters which resulted in the lowest overall RMS error during the 20-50 keV validation mention above. The third panel was generated with the input parameters giving the best results in the midnight-to-dawn local time sector so important to spacecraft charging. We expect the spacecraft to charge negatively when this current density is greater than zero. Notice that the maximum calculated charging current occurs for all three runs of Day 215 during the period when DSCS III charged to -600 V. For all three input parameter variations, the relative timing of the net current increases near the charging period time follow patterns similar to those associated with the arrival of the 20-50 keV electrons. While the Kp -Only run produces the largest charging current densities, they arrive early. The arrival timing is better in the other two runs, but currents are also weaker. The calculated charging current density on Day 45 (not shown) is very similar to that for Day 215, though DSCS III only charged to -300 V on that day. No charging current is calculated for Day 217 when DSCS III charged to -200 V (also not shown).

In the case of the large storm run covering days 123 and 124 of 1998, charging currents larger than those shown in the upper panel of Figure 2 were calculated even though no charging was observed. The MSM indicates that the dayside magnetopause may have crossed inside geosynchronous altitude. This large compound dynamic event is, of course, the very type that spacecraft operators are most interested in and also the most difficult to model. While some aspects of spacecraft charging can be statistically correlated with geomagnetic indices⁸, this event demonstrates the need for simulations to track the time evolution

As seen in Figure 2, the net charging current is always very small compared to the incident electron current due to secondary, backscatter, and ion currents. The net charging current is less than 10% of the incident electron current. All the other contributions to the net current (secondary and backscattered electrons, and incident H^+ and O^+ ions) are of the opposite sign from the incident electron current. In all cases, the presence of charging current densities derived from the MSM simulations seems to be associated with an increase in the ratio of high to low energy electrons and often a concurrent decrease in the ion population. Both conditions occur regularly in the midnight to dawn local time sector where spacecraft charging is most frequently observed.

Conclusions

The MSM still holds promise as a contributor to an effective spacecraft charging forecast tool. This work should help us to refine our expectations in this regard. Driving the MSM with a variety of input parameter combinations demonstrated that the basic behavior of the model is still consistent with the requirements of producing particle environment input for charging algorithms. Specifically, environment models should be able to demonstrate the ability to offer a realistic specification of electron and ion fluxes, and more importantly, the changes in their respective spectra that determine backscatter and secondary electron yields. Our simple method of using instantaneous, inferred current densities as the charging metric for a minimum spacecraft description, of course, represents a very gross approximation to a very complex time dependent problem. It does, however, provide leads as to how we might best utilize the model. For example, simulations using different driving parameters show different strengths. A straightforward Kp -dependent charging algorithm would likely result in comparatively higher charging current densities that tend to arrive earlier than observed. Linkage with a Kp forecast algorithm based on solar wind measurements⁹, however, would result in a true forecast capability. On the other hand, other input parameter selections provide better arrival timing for certain local time sectors but tend to result in weaker charging. The final answer might involve using a composite model depending on the geophysical conditions and the local time sector of primary interest.

References

- [1] Katz, I., V A Davis, M Mandell, D Cooke, R Hilmer, L H Krause, Forecasting satellite charging: Combining space weather and spacecraft charging, 38th AIAA Aerospace Sciences Meeting, Reno NV, 10-13 January 2000, *AIAA-2000-0369*, 2000
- [2] Hilmer and Ginet, A Magnetospheric Specification Model Validation Study: Geosynchronous Electrons, *J. Atmos. and Solar-Terr. Phys.*, 62, 1275-1294, 2000
- [3] Mullen, E.G., A.R. Frederickson, G.P. Murphy, K.P. Ray, E.G. Holeman, D.E. Delorey, R. Robson, M. Farar, "An Autonomous Charge Control System at Geosynchronous Altitude: Flight Results for Spacecraft Design Consideration," *IEEE Trans. Nucl. Sci.*, NS-44, 2188, 1997

- [4] Lambour, R L, L A Weiss, R C Elphic, M F Thomsen, Global modelling of the plasmasphere following storm sudden commencements, *J. Geophys. Res.*, 102, 24351, 1997
- [5] Heppner, J P, and N C Maynard, Empirical high-latitude electric field models, *J. Geophys. Res.*, 92, 4467, 1987
- [6] Hilmer, R V, and G-H Voigt, A magnetospheric magnetic field model with flexible current systems driven by independent physical parameters, *J. Geophys. Res.*, 100, 5613, 1995
- [7] Katz, I., J.J. Cassidy, M.J. Mandell, G.W. Schnuelle, P.G. Steen, J.C. Roche, "The Capabilities of the NASA Charging Analyzer Program, Spacecraft Charging Technology – 1978," NASA CP-2071, AFGL-TR-79-0082, edited by R.C. Fincke and C.P. Pike, p. 101, 1979
- [8] Krause, L H, B K Dichter, D J Knipp, and K P Ray, The relationship between DSCS III sunlit surface charging and geomagnetic activity, *IEEE Trans. Nucl. Sci.*, NS-47, 2224, 2000
- [9] Detman, T and J Joselyn, Real-time K_p predictions from ACE real time solar wind, in Proceeding of Solar Wind 9 Conference, Oct. 5-9, 1998, Nantucket Island, MA

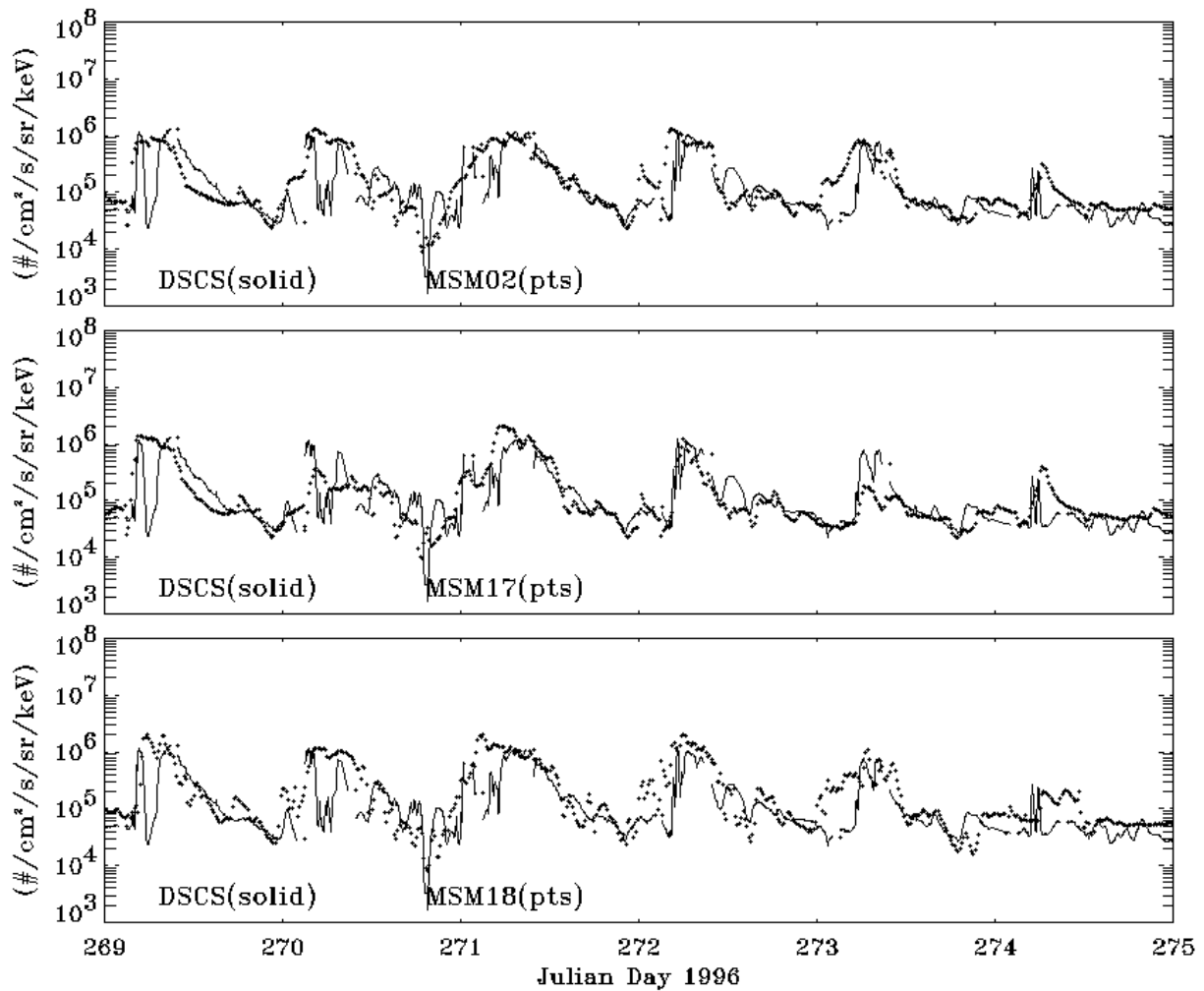


Figure 1. Electron flux (20–50 keV) specified by MSM (points) and measured by DSCS (line) for six days in 1996 (DSCS crosses 0 LT at 0330 UT). Shown are results from three MSM runs driven by different input sets (see text for details).

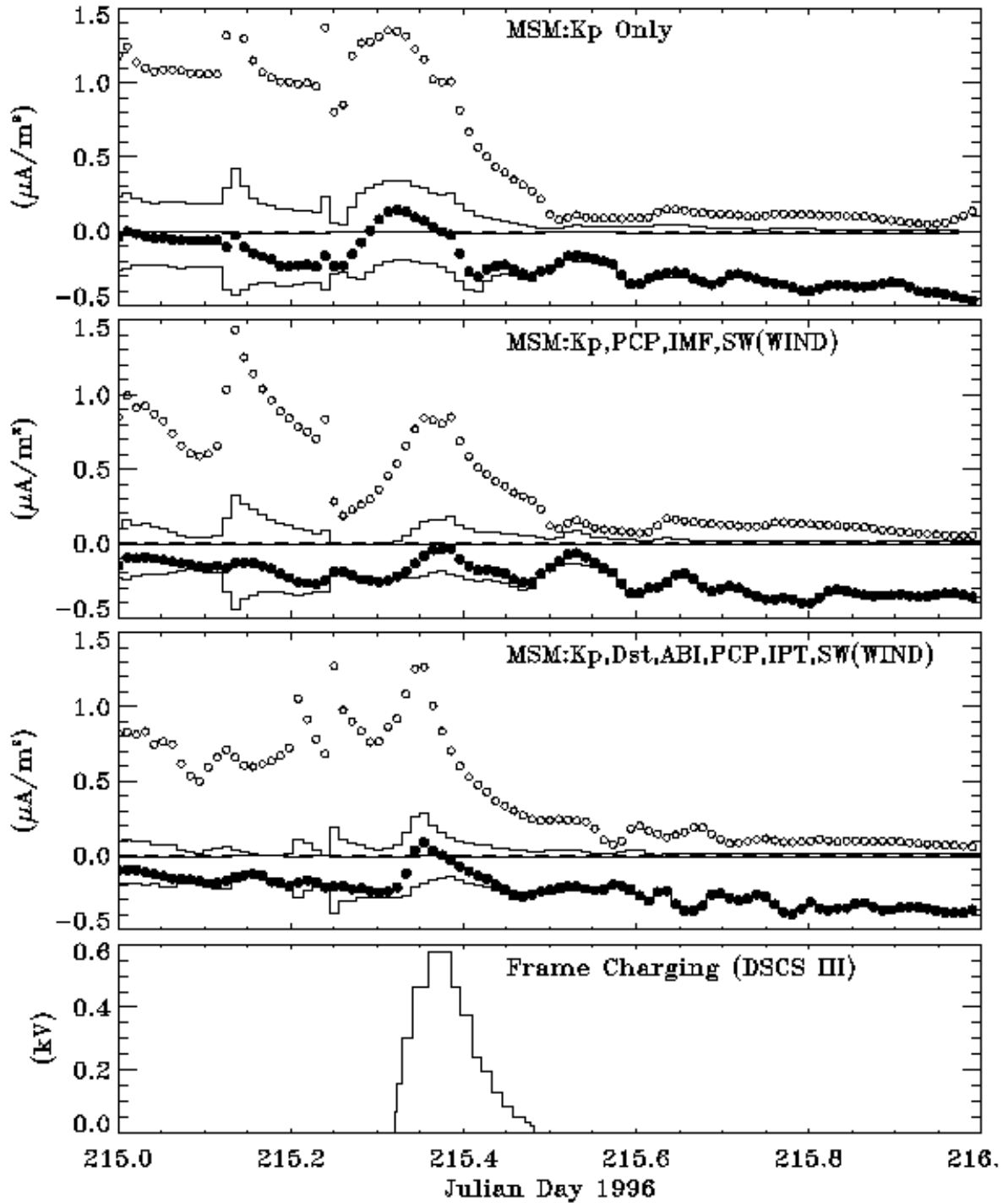


Figure 2. MSM generated current densities from three input parameter combinations (top panels) with flight data showing DSCS spacecraft charging (bottom panel). The effect of the incident electron current density (circles) is reduced by backscatter and secondaries to give the positive current density histograms. Incident H+ plus related secondary electrons result in the negative current density histograms. The net charging current density (dots) also includes contributions from incident O+ and related secondary electrons.